

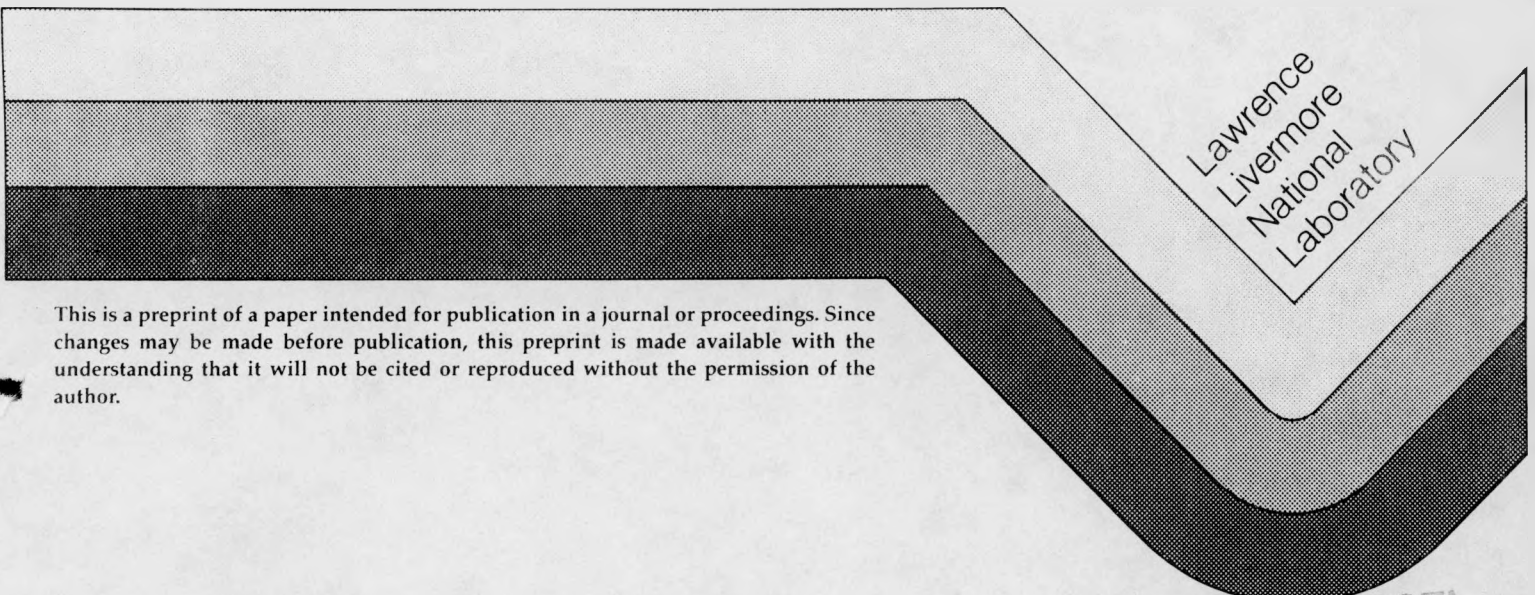
UCRL- 102305
PREPRINT

COMPUTING SHOCK WAVES IN TURBULENT MIXING REGIONS

Alfred C. Buckingham

This is a preprint of a paper to be presented and published
as part of the Proceedings of the 7th Biennial Nuclear
Explosives Design Physics Conference, LLNL, Livermore
~~November~~, 1989
Oct

November 1989



Lawrence
Livermore
National
Laboratory

This is a preprint of a paper intended for publication in a journal or proceedings. Since changes may be made before publication, this preprint is made available with the understanding that it will not be cited or reproduced without the permission of the author.

Received by OSTI

JAN 26 1990

DISTRIBUTION OF THIS DOCUMENT IS UNLIMITED

DISCLAIMER

This report was prepared as an account of work sponsored by an agency of the United States Government. Neither the United States Government nor any agency thereof, nor any of their employees, makes any warranty, express or implied, or assumes any legal liability or responsibility for the accuracy, completeness, or usefulness of any information, apparatus, product, or process disclosed, or represents that its use would not infringe privately owned rights. Reference herein to any specific commercial product, process, or service by trade name, trademark, manufacturer, or otherwise does not necessarily constitute or imply its endorsement, recommendation, or favoring by the United States Government or any agency thereof. The views and opinions of authors expressed herein do not necessarily state or reflect those of the United States Government or any agency thereof.

DISCLAIMER

Portions of this document may be illegible in electronic image products. Images are produced from the best available original document.

COMPUTING SHOCK WAVES IN TURBULENT MIXING REGIONS

Alfred C. Buckingham

Center for Compressible Turbulence, Lawrence Livermore National Laboratory,
University of California, Livermore, California 94550, USA

ABSTRACT

This concerns the observed random changes to shock transitional velocity, density, and temperature induced when shocks interact with turbulence. This interaction may be useful as a diagnostic for ascertaining the distribution of interaction energy between competitive acoustic, entropy and vortical modes. Numerical procedures are used here to supplement physical experiments. The results are obtained from use of an "ALE" finite-difference code method with visco-elasticity (SHALE), a hybrid Euler/Lagrange pseudospectral method, and a Monte-Carlo random-choice procedure. The latter magnifies the shock front transition region generating PDF-transition profiles.

I. INTRODUCTION

In this work, numerical simulations and analyses are used to expand shockwave dimensions that are too small or time intervals too brief to permit adequate experimental access and resolution. The numerical results trace the evolution of structure (velocity, temperature, density profiles) within a spatially and temporally distorted shock front. Shock distortions develop as the shock front advances through and interacts with upstream turbulence. Experiments are used to help verify that the simulations provide, at least, reasonable representations of ensemble averages of a collection of individual shock turbulence interaction realizations.

This work continues previous analyses on the interaction of shock waves with turbulence.⁽¹⁾ Much of the present discussion is based on a recent publication which outlines the numerical procedures developed for this analysis.⁽²⁾ Conceptually, shock-wave interactions couple directed shockwave translational energy into turbulence kinetic energy during shock transition. The intensity of the turbulence is amplified and its spectra altered. The changes to the turbulence characteristics are most apparent when relatively low Mach Number shockwaves encounter strong turbulence. However, some evidence and considerable theoretical speculation suggests that significant shock enhancement of turbulence may be evident at higher Mach Numbers.

II. SHOCK WAVE TURBULENCE AMPLIFICATION

Figure 1 illustrates pseudospectral transform method results, using two forms of imbedded shock numerical methods. The figure illustrates the amplification of the initial rms turbulence velocity, $\langle u_1' \rangle$, when a plane shock intersects a turbulent field at an incident angle, $\theta = 30^\circ$. The amplified turbulent velocity, after-shock interaction is $\langle u_2' \rangle$. It is seen to increase with shock Mach Number, M_∞ . The more accurate of the numerical results shown

were developed at the cost of additional analytical and computer effort, using dynamic near shock-front mesh refinement and shock fitting. Linear theory (solid line) results are plotted for comparison.⁽³⁾ A cross-hatched envelope bounding experimental shockwave boundary layer and reflected shockwave interaction (shock tube) results also are shown to provide perspective.

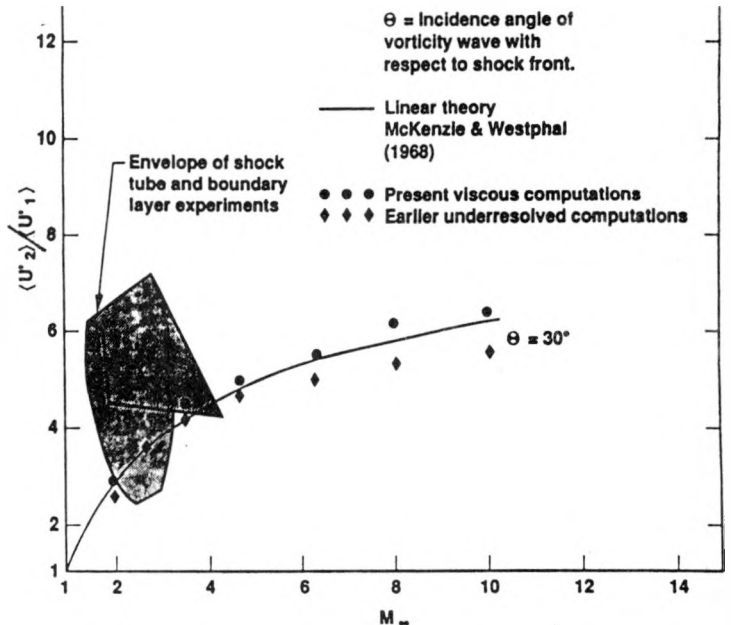


Fig. 1. Amplification of turbulence intensity by interactive passage of shock-wave; numerical and experimental results.

III. SHOCK STRUCTURE

Almost 80 years ago, Taylor⁽⁴⁾ illustrated that, to leading order, the shock-front thickness depends directly on the statistically averaged molecular transport properties and inversely on the shock strength and gas density. The present calculations indicate

MASTER

DISTRIBUTION OF THIS DOCUMENT IS UNLIMITED

that we might expect analogous influence on shock thickness, if we examine the turbulent eddy exchange processes in place of Taylor's molecular-scale transport distributions.

However, more accurate estimates of the energy partition that develops between advancing shock and turbulent field require consideration of higher-than-leading-order interactions. Strong coupling must be properly accounted for between all three competing modes (entropy, vorticity, acoustic). Kovaszny's (5) seminal analysis of almost 35 years ago implies that strong interactive coupling first emerges at the third-order terms in an asymptotic expansion. To examine this, asymptotic analysis is applied in combination with numerical results to help resolve the details of the interaction.

The asymptotic matching results in a compressible series expansion of functions depending on acoustic (a), entropy (\bar{s}), and vorticity ($\underline{\omega}$) modes. To third order, the shock thickness, δ_s^T is given by an asymptotic series of the form

$$\begin{aligned} \delta_s^T = & A_1 \epsilon_{\perp} v_e \left(\langle u \rangle, \lambda_M \right) \\ & + A_2 \epsilon_{\perp}^2 v_e \left(\langle u \rangle, \lambda_M, A_3 a + A_4 \bar{s} + A_5 \underline{\omega} + \dots \right) \\ & + A_6 \epsilon_{\perp}^3 v_e \left(\langle u \rangle, \lambda_{M1}, A_7 F(a, \bar{s}, \underline{\omega}, \dots) \right). \end{aligned} \quad (1)$$

Here, $\epsilon_{\perp} = \rho_- / \rho_+$, is the reciprocal of the shock transition density jump and serves as the small parameter in the expansion. Interactive coupling of modes occurs at the third order in the functions, F. The principal length scale, λ_M , is effectively a "mixing length" which is developed from the numerical shock structure simulations in the absence of adequate experimental results.

Examination of the developed attributes and implications of the asymptotic analysis is extensively discussed in a separate paper currently in preparation. (6)

IV. RANDOM CHOICE SHOCK-FRONT DESCRIPTION

A random selection Monte-Carlo procedure is used to develop the perturbation distribution functions normal to the advancing shock surface in association with a spectral collocation procedure, applied spanwise, to represent the tangential flow influence of the distortions along the shock. The simulated distortions are created by interactions with modeled upstream random disturbances. Inspired by Taylor's (4) molecular shock-structure concept and the later extensions by Mott-Smith (7) approximating the shock-front velocity exchanges by linearized combination of upstream, and downstream velocity distributions; we develop the requisite turbulent eddy influences on the shock-structure distribution functions parallel to shock-propagation

direction. The procedure is based on Bird's (8) Monte-Carlo kinetic theory shock-wave computations.

Linearized integral combination of random valued fluxes of mass, momentum and energy, evaluated about preshock (subscript, 0) and postshock (subscript, 1) turbulent field produce a streamwise (ξ), integral finite shock thickness. Velocity and exchange scalar flux distributions are computed at a series of vertical locations (η) along the distorted shock-front surface.

At this approximation level, we define the mean shockwave velocity, \bar{u}_N , with zero variance. Random flux exchange integrand contributions, $\phi'_{(i)} - \phi'_{(1)}$ are defined for the streamwise shock transition realization computations, based on assumed (turbulent) randomness of both preshock and postshock material velocity components:

$$\vec{q}_{(i)} = \langle \vec{q}_{(i)} \rangle (\text{Mean}) + \vec{q}'_{(i)} (\text{Perturbational}), \quad (2)$$

where

$$\vec{q}_{(i)}^2 = u_{(i)}^2 + v_{(i)}^2, \quad (3)$$

$$u_{(i)} = \frac{d\xi}{dt}, \quad v_{(i)} = \frac{d\eta}{dt},$$

and

$$\phi'_{(i)} = \left(u'_{(i)} - \bar{u}_N \right). \quad (4)$$

To represent the collective random flux exchanges, the transition realization (ξ wise) contributions to the integrals of mass, momentum and energy are formed. These are identified by the symbol, \tilde{J} . In addition to the random velocities, we also identify transported passive scalars: density (ρ), internal energy density (e), and through an appropriate equation of state, the pressure (p), viz.

$$\rho(\xi) = \rho(\rho, \theta). \quad (5)$$

In the test calculations, an ideal gas equation of state was used, with the polytropic exponents, 7/5 (conventional) or 5/3 (turbulent "model" gas) assigned. \tilde{J} contributions are evaluated on integration over a finite shock width, δ_s (to be determined). Conditionally, conservation requires that, over the integral range, $[\xi - \delta_s/2, \xi + \delta_s/2]$,

$$\vec{J} = \begin{bmatrix} dM(\xi) = \rho_0 \phi'_0 - \rho_1 \phi'_1 & \text{(Mass)} \\ dMu(\xi) = (\rho_0 u'_0 \phi'_0 - \rho_1 u'_1 \phi'_1 + p'_0 - p'_1) & \text{(Momentum)} \\ dME(\xi) = \rho_0 q_0 \phi'_0 - \rho_1 q_1 \phi'_1 + 2(\rho_0 \theta_0 \phi'_0 - \rho_1 \theta_1 \phi'_1) \\ \quad + 2(\rho_0 u'_0 - \rho_1 u'_1) & \text{(Energy)} \end{bmatrix} \quad (6)$$

The discontinuous, mean shock jump conditions are met as an integral constraint.

$$\int_{\xi-\delta/2}^{\xi+\delta/2} \vec{J} d\xi = 0 \quad (7)$$

To complete the system for integration, a global constraint on the tangential material velocity, that is exact in a stationary system, is applied in accord with central limit considerations for the random velocity field,

$$v_0 = v_1, \text{ viz., one invokes} \\ \vec{q}_i = \langle q_i \rangle, i = 0, 1. \quad (8)$$

Equilibrium molecular thermodynamic consistency is assumed, permitting Eqn. (5) to represent the state globally.

Each of the distortions along the shock front contributes both streamwise and tangential (parallel to the vertical axis) perturbational components. The contributions of the ensemble of realizations over the entire surface is effectively combined by computing momentum, mass, and energy integrals over the two dimensions of a finite-thickness shock surface. The normal integrations include derivatives of both tangential and streamwise fluxes evaluated in phase space then transformed back to configuration space using an FFT collocation procedure.

The stationary values of the tangential derivatives are obtained by applying the influence of distorted shock geometric surface functions. The surface functions, Λ , must be continuous and analytic, at least through second derivatives,

$$\vec{J} = \vec{J}(\Lambda, \Lambda, \Lambda, \Lambda, \Lambda, \Lambda, \vec{q}, \rho, e), \quad (9)$$

to satisfy consistency and realizability of vorticity evolution at the continuously distorted shock surface.

Each random exchange distribution is considered a single, instantaneous realization for the streamwise ξ distribution profiles and consequent integral-length scales. Figures 2 and 3 show a superposition of realizations taken at randomly selected shock surface (η) levels. The separately computed, distorted shock-front surface is shown as a shock-front silhouette on the

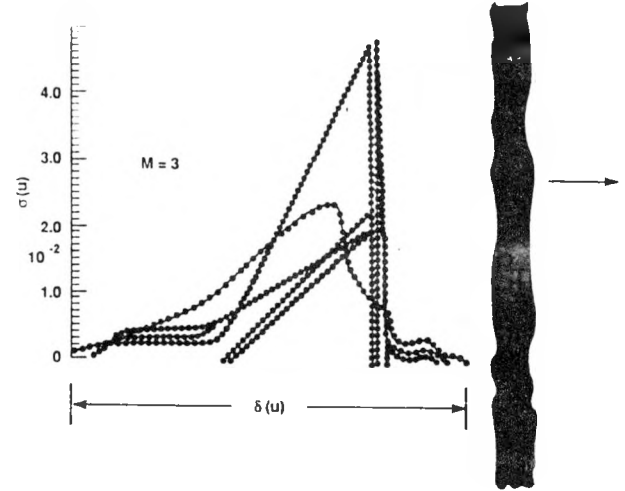


Fig. 2. Velocity standard deviation for several realizations taken at various positions along the turbulence distorted shockfront shown as a silhouette ($M_S=3.0$).

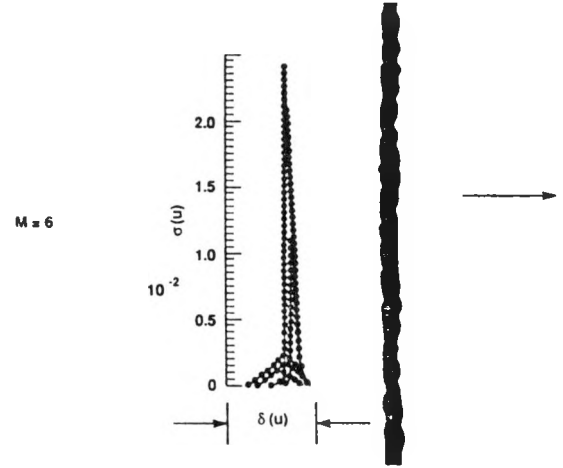


Fig. 3. Velocity standard deviation for several realizations taken at various positions along the turbulence distorted shockfront shown as a silhouette ($M_S=6.0$).

right. Figures 3 and 4 are developed from results at shock Mach Numbers of 3 and 6, respectively. The distorted shock fronts are obtained separately from pseudospectral collocation calculations (9) or discrete Lagrange/Euler SHALE calculations.(10)

V. VISCO-ELASTIC RESPONSE

Emphasis also is placed on the modeling of the turbulent-field response to shock transition with a kinematic model. The model form should permit efficient implementation and application in existing computer codes for prediction of the shock-turbulent amplification process, and its temporal persistence after the shock front moves away.

Current attention has been placed on a linear visco-elastic response model for the shock-amplified turbulent process. Its relationship to the dynamic response and relaxation of the turbulent field, as well as its relationship to artificial "viscous" damping term(s) used with shock-capturing schemes on discrete mesh simulations, are currently under study.

Figure 4 illustrates the apparent redistribution of turbulence kinetic energy based on the random choice procedure averages in comparison to a visco-elastic response model applied at the shock wave. In addition, we show results of a kappa-epsilon conventional turbulence single-point closure model and a more or less conventional shock oscillation damping artificial viscosity model, "Q". All results are remapped to a common shock thickness, Δ_s , to assist comparison.

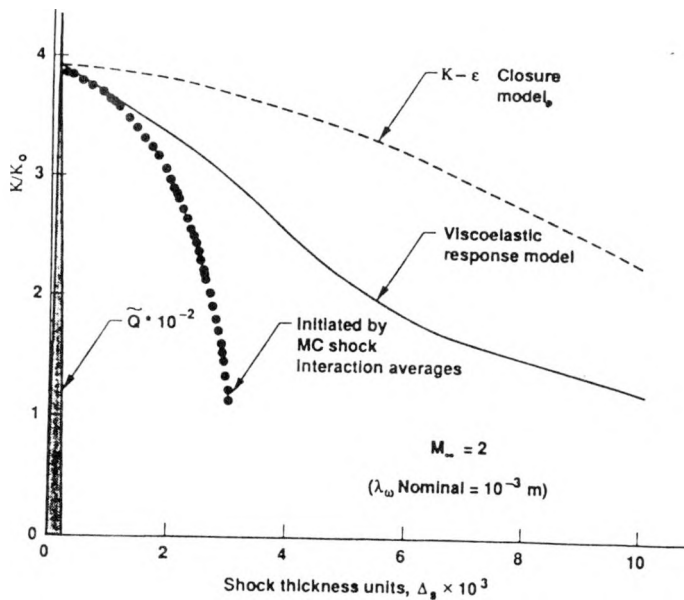


Fig. 4. Comparison of turbulent kinetic energy profiles through shock transition as predicted by Monte Carlo results, visco-elastic response model results, and simple application of an artificial viscosity, Q, model. Mach No. = 2.0.

response model results, and simple application of an artificial viscosity, Q, model. Mach No. = 3.5.

Figure 5 repeats the numerical simulation (experiment) initiated in Fig. 4, but for a stronger $M_\infty = 3.5$ shock strength. Results currently have been obtained for analysis up to a Mach Number of 8.

VI. CONCLUSIONS

The effects of Mach Number appear to favor a coalescence of interaction times and length scales between entropy, vorticity, and acoustic modes with increasing Mach Number for energy transfer in shock-turbulence interaction. This convergence of scale sizes, however, probably does not persist indefinitely and,

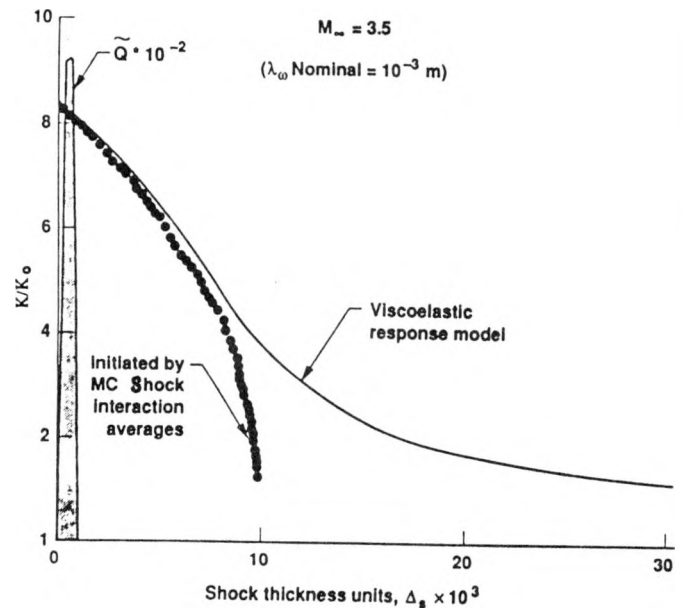


Fig. 5. Comparison of turbulent kinetic energy profiles through shock transition as predicted by Monte Carlo results, visco-elastic response model results, and simple application of an artificial viscosity, Q, model. Mach No. = 3.5.

in fact, our analysis indicates a divergence of scale sizes in the hypersonic ($M \geq 6$) range.

The corresponding amplification rates increase less and less with increasing Mach Number and, perhaps, diminish at high Mach Numbers to distinct limiting values.

The persistence or duration of the shockwave-to-turbulence amplification influence seems to drop off with increasing Mach Number and increasing Reynolds Number.

A turbulent subgrid closure model may overcompensate for Q in shock-damping, but may be a closer representation of nature if both dilatational and deformational components in viscosity are included in the shock-front explicit damping model. Linear visco-elasticity appears to be appropriate for modeling the interactive response between shock and turbulence.

VII. ACKNOWLEDGMENTS

This is a report of research conducted under the auspices of the U.S. Department of Energy by the Lawrence Livermore National Laboratory under Contract No. W-7405-ENG-48.

VIII. REFERENCES

1. Buckingham, A.C., *Numerical Methods in Laminar and Turbulent Flow*, V, Part 2, ed. C. Taylor, Pineridge Press, Swansea, UK, (1987), pp. 963-974.
2. Buckingham, A.C., *Numerical Methods in Laminar and Turbulent Flow*; VI, Part 1, eds. C. Taylor, P. Gresho,

- R.L. Sani, J. Häuser, Pineridge Press, Swansea UK (1989), pp. 805-814.
3. McKenzie, J.F., K.O. Westphal, *PHYSICS OF FLUIDS*, **11**, (11), (1968), pp. 2350-2362.
 4. Taylor, G.I., *Proc. Royal Society London, A*, **84**, (1910), pp.371-377.
 5. Kovasznay, L.S.G., *J. AERO. SCI.*, **20**, (10), (1953), pp. 657-682.
 6. Buckingham, A.C., *Asymptotic Analysis of Modal Coupling in Compressible Shock Turbulence Interaction*, in preparation for submission to *PHYSICS OF FLUIDS* (1989).
 7. Mott-Smith, H.M., *PHYS. REVIEW*, **82**, (1951), 885.
 8. Bird, G.A., *J. FLUID MECH.*, **30**, (1967), pp. 479-487.
 9. Buckingham, A.C., *41st Annual Mtg, Div. of Fluidynamics, American Physical Society*, State Univ. of New York, Buffalo NY, (1988).
 10. Demuth, R.B., L.G. Margolin B.D. Nichols, T.F. Adams, B.W. Smith, *SHALE: A Computer Program for Solid Dynamics*, Los Alamos National Laboratory, LA-10236, Los Alamos NM (1985), and informal documentation, communications with L.G. Margolin on modifications to the fluidynamic version SHALE code, Lawrence Livermore National Laboratory, Livermore CA, (1988-1989).